SCIENCE DILIMAN
Received October 14, 1991

Development of a Storm Surge Prediction Model

Paul C. Rivera and Jorge G. Delas Alas*
Department of Meteorology and Oceanography
College of Science

ABSTRACT

A numerical model based on the depth-integrated hydrodynamical equations is formulated. It is used to study the response of an ideal ocean shelf region of limited areal extent subjected to the passage of hypothetical cyclones (symmetric and asymmetric) with known characteristics. Four sets of numerical experiments are conducted to investigate storm surges generated within the model basin. The first set considers the effect of varying cyclone directions of approach relative to the basin on the resulting storm surge. The second set considers the effect of varying cyclone speeds and sizes, the third on the effect of varying shelf widths, and the fourth on the effect of asymmetry in the cyclone wind field. Results for the seven cyclone directions investigated showed potential surge threats for cyclones that made landfall to the right or center of the model basin. The highest magnitude of surges was generated by a cyclone which crossed the basin and made landfall at the center of the coastline. The effect of the cyclone speed did not matter much in the peak surge generated, whereas the effect of the cyclone size was significant. Furthermore, the effect of varying shelf widths clearly demonstrated the reduced effect of the surface stress in deeper waters. Lastly, the asymmetry of the cyclone wind field has a substantial effect on the magnitudes of surges generated.

INTRODUCTION

A transient phenomenon observed on the sea during the passage of tropical cyclones is the storm surge which is the abnormal rise of the sea surface directly caused by the time and space variations of the wind and pressure fields associated with the cyclone. In contrast to surface waves which have periods of only a few seconds and wavelengths of several meters, a surge has a wavelength scaled in kilometers (approximately 4 times the storm

* Author to whom correspondence should be addressed.

radius of maximum wind) and with a period dependent on the speed of storm movement. It has typically a duration of several hours but sometimes lasts for a few days affecting more than a hundred kilometers of coastline.

In particular, a surge is noticeable on shallow continental shelves where the tangential winds around a cyclone are most effective in inducing shearing stresses that drive the sea into motion. A surge can be very disastrous particularly when it inundates low-lying areas farther away from the coast. In fact, it can be considered as one of the world's foremost natural hazards as far as loss of life and property damage are concerned. This was proven by the storm surge in November 1970 which occured in the shallow Bay of Bengal and killed more than 300,000 people in Bangladesh (Murty et al., 1986). A major surge was driven inland by the cyclone inundating low-lying areas which resulted in the mass killing and destruction. It is considered to be the most devastating surge of this century.

The Philippines has been known to be a surge-prone area. The warm waters of the western Pacific Ocean is a good breeding ground of tropical cyclones, and as these cyclones move westward or north westward towards the archipelago, they generate surges of varying amplitudes in the eastern coasts of the Philippines and other shallow coastal areas. Considerable damage has also been caused by these phenomena in the country.

Prediction of the occurrence of storm surges is very important considering the potential danger posed by this natural coastal phenomenon. Indeed it has caused so many deaths and enormous economic damage and the only practicable counter-measures are improved surge warning systems and construction of coastal defences along frequently flooded low-lying coastal areas. The construction of adequate coastal defences is at present not feasible owing to economic and technical constraints. An improved surge warning system is the alternative, hence a more intense study on the prediction of storm surges is necessary.

This study is not only useful in the natural disaster mitigation program of the country. Estimation of peak water levels during the passage of tropical cyclones is of great importance in off shore and coastal engineering particularly in the design of coastal structures.

Prediction of storm surges in the Philippines using a numerical-dynamical technique begins with the works of De las Alas and Encarnacion (1984). They have a one-dimensional numerical model based on the depth-integrated hydrodynamic equations that includes the non-linear advective terms. The model developed appeared successful in predicting peak surges that occurred in some coastal areas in the country. Martin (1985) has a similar model for Manila Bay. This time it is two dimensional but does not include the non-linear advective terms. The set of predictive equations is solved in a staggered fashion with the driving force approximated by a theoretical wind field suggested by Jelesnianski (1965).

MODEL DESCRIPTION

The mathematical model described here makes use of the depth-integrated equations of motion and mass continuity which can be written as

$$\frac{aU}{at} + \frac{a}{ax}\left(\frac{U^2}{h+\zeta}\right) + \frac{a}{ay}\left(\frac{UV}{h+\zeta}\right) = fV - \frac{(h+\zeta)}{p}\frac{ap^a}{ax} - g\,(h+\zeta)\,\frac{a\zeta}{ax} + \frac{1}{p}\left(\tau^x{}_s - \tau^x{}_b\right) \quad (1)$$

$$\frac{aV}{at} + \frac{a}{ax}\left(\frac{UV}{h+\zeta}\right) + \frac{a}{ay}\left(\frac{V^2}{h+\zeta}\right) = -fU - \frac{(h+\zeta)}{p}\frac{ap^a}{ay} - g\,(h+\zeta)\,\frac{a\zeta}{ay} + \frac{1}{p}\left(\tau^y{}_s - \tau^y{}_b\right) \quad (2)$$

$$\frac{a\zeta}{at} + \frac{aU}{ax} + \frac{aV}{ay} = 0 \quad (3)$$

where

U, V = the horizontal components of the vertically integrated current (transport vector) in the x and y directions, respectively

ζ = the sea surface elevation (surge height)

h = the depth of the undisturbed sea level

g = the acceleration due to gravity

p = the sea water density

p^a = the atmospheric pressure above the sea surface

τ_s = the wind stress at the sea surface

τ_b = the bottom stress.

In general, equations (1)–(3) described the dynamics of storm surges and tides alike in a barotropic ocean of limited areal extent so that curvature of the earth's surface is neglected. These equations yield the values of the dependent variables U, V and ς as functions of space and time. Given the pressure and stress forcings from a cyclone, the sea surface elevation ς (surge heights in particular) and the transport components U and V can be predicted in a sea region of finite areal extent with sufficient accuracy.

Dynamically, the vertically integrated equations of motion equate the total acceleration of the sea water (in the left side) to the forces acting on it (in the right) namely; the coriolis force, the pressure gradient forces (atmospheric and surface slope contributions), and the surface stress. As one, they express conservation of momentum. The depth-integrated continuity equation expresses conservation of fluid mass, i.e. in a vertical column of sea water, equation (3) implies that a change in the sea surface elevation ζ associated with the storm surge is balanced by the inflow and outflow of sea water through its sides.

The predictive equations are simplified by eliminating the non-linear advective terms. Also, the effect of the atmospheric pressure is excluded since there is negligible horizontal pressure gradients in a relatively small area of prediction. Thus the predictive equations become

$$\frac{a\,u}{a\,t} = fV - gh\,\frac{a\,\zeta}{a\,x} + \frac{1}{p}\left(\tau^{x}_{s} - \tau^{x}_{b}\right) \tag{4}$$

$$\frac{a\,V}{a\,t} = -\,fU - gh\,\frac{a\,\zeta}{a\,y} + \frac{1}{p}\left(\tau^{y}_{s} - \tau^{y}_{b}\right) \tag{5}$$

$$\frac{a\,\zeta}{a\,t} + \frac{a\,U}{a\,x} + \frac{a\,V}{a\,y} = 0. \tag{6}$$

The surface stress, τ_5, being the main forcing in the surge model is computed using the conventional quadratic law given by

$$\tau_s = p_a c_d \,|W|\, W \tag{7}$$

where p_a is the air density and c_d is a drag coefficient which is allowed to vary with the wind speed as in

$$c_d = (0.8 + 0.065\,|W|)\ x\ 10^{-3} \tag{8}$$

The magnitude of the wind vector $|W|$ should be in m/s (Wu, 1982).

On the other hand, the bottom stress τ_b is computed using a linear law as in Dela Alas et al. (1984). It is given by

$$\tau_b(x,y) = k\,\frac{(U,V)}{h} \tag{9}$$

where k is the bottom friction coefficient assumed constant. The value which yields reasonable results in the numerical experiments is 2.4 x 10^{-3} and this is adopted for all the succeeding experiments.

The wind speed, W, is specified using Jelesnianski's typhoon model i.e.,

$$W = W_r \left(\frac{r}{R}\right)^{3/2}, \qquad 0 \leq r \leq R \tag{10}$$

$$W = W_r \left(\frac{R}{r}\right)^{1/2}, \qquad r \geq R \tag{11}$$

Figure 1 shows the wind speed W as a function of distance r around the cyclone center.

Including the effect of the inflow angle ϕ, the stress components are then computed using

$$\tau^x_s = p_a c_d\, W^2_R\, \frac{r^2}{R^3}\, A$$

$$\tau^y_s = p_a c_d\, W^2_R\, \frac{r^2}{R^3}\, B, \qquad 0 \leq r \leq R \tag{12}$$

$$\tau^x_s = \rho_a c_d \; W^2_R \frac{R}{r^2} \; A$$

$$\tau^y_s = \rho_a c_d \; W^2_R \frac{R}{r^2} \; B, \qquad r \geq R \tag{13}$$

where

$$A = -y \cos\phi - x \sin\phi \text{ and } B = x \cos\phi - y \sin\phi .$$

An asymmetric hypothetical cyclone is also tested in the present study. The asymmetry is introduced simply by adding vectorially the speed of the cyclone's translational motion to the component of the radial wind parallel to its direction of motion to confine stronger winds to the right of the cyclone's direction of motion (as most observations show).

Solution of eqs. (4)–(6) is obtained using finite difference technique. Temporal derivatives are approximated by forward-time and space derivatives by a slightly staggered fashion using the Arakawa B-grid. This has the obvious advantage of treating computational boundaries easily, particularly the coastal boundary where the ζ's need not be specified. Values at the two lateral boundaries are computed using the method of characteristics described by Roed and Cooper (1987). Again, only the transport components here need to be specified. For the right and left open boundaries, respectively, these are given by

$$\frac{\partial U}{\partial t} = fV + \frac{1}{\rho}\left(\tau^x_s - \tau^y_b\right) + \frac{C_0}{2}\frac{\partial}{\partial x}\left(U + C_0\,\zeta\right) \tag{14}$$

$$\frac{\partial U}{\partial t} = fV + \frac{1}{\rho}\left(\tau^x_s - \tau^y_b\right) + \frac{C_0}{2}\frac{\partial}{\partial x}\left(U - C_0\,\zeta\right) \tag{15}$$

where C_0 which is equal $\sqrt{gh}$ is the phase speed of a long gravity wave. The y-component (V) is specified using a zero-gradient condition. At the coastal boundary, the values of the transport component normal to it are set to zero throughout the integration period, whereas the tangential component is computed using the momentum equation. For the open sea boundary where only the surge heights need be specified, it is assumed that the sea surface is flat. The surge heights are set to zero throughout the integration period.

MODEL RESULTS

The model equations are integrated for a period of 24 hours to yield values of the depth-integrated current and surge heights in a variable depth basin of relatively small areal extent with a straight coastline. The lateral boundaries with the seaward end are assumed open. The numerical experiments conducted make use of various numerical constants. These include the location of the computational domain at latitude 15°N, assigning a constant value to the cyclone's inflow angle of 15°, a maximum wind of 60 m/s and a radius of maximum wind of 30 kms for the hypothetical cyclone used.

The results of the model for six generalized typhoon tracks investigated showed potential surge threats especially for cyclones that crossed the model basin. These are presented in terms of time-history plots in Figures 2 to 4. The highest magnitude of surges being 2.8 m (in these experiments), is generated by a cyclone which moved at normal incidence to the coast and made landfall at the center of the coastline of the model basin. This is shown in Figure 2. In agreement with theory and observa tion, the modeled maximum surges occur more or less during landfall time as shown. Landfall time is indicated by the typhoon symbol. Note that all the plotted surges are taken to the right of landfall (observer at sea facing land) particularly at the point of maximum winds. This is done to assess the maximum surges which may occur in the basin.

The effect of the cyclone speed (in so far as the maximum speed being taken here is considered, i.e. 7 m/s) does not matter very much in the peak surge generated as can be seen in Figure 5a, except for the durations of the surge occurrence. However, it is speculated that further increase of the cyclone speed would cause higher surges most especially when this speed matches the phase speeds of the surges generated (observations support this). On the other hand, the effect of cyclone size is found to be significant in that much higher surge was generated by a large cyclone (40 km radius) than a small one (20 km radius). This can be seen in Figure 5b. The effect of varying shelf width (smaller shelf width implying deeper basin) on the surges generated demonstrated the reduced surface stress effect on a deep basin where smaller amplitudes of surges were generated as shown in Figure

6. Lastly, the asymmetry of the cyclone wind field with stronger winds to the right of the cyclone direction of motion produced substantial effect on the peak surge generated particularly when the cyclone crossed the center of the basin. The effect of asymmetry is shown in Figure 7.

CONCLUSION

A numerical-dynamical model based on the linearized depth-integrated hydrodynamical equations has been developed to predict the occurrence of storm surges. A hypothetical basin is used and a typhoon of known characteristics is allowed to pass over it in predefined directions. Several numerical experiments are conducted to investigate storm surges generated in the basin.

In general, though the model is simplified by the elimination of the effects of advection and atmospheric pressure force, it is able to simulate fairly well the storm surge phenomenon as revealed by the model results. In particular, the time evolution as well as the spatial distribution of the surge is well in agreement with theory and observations.

REFERENCES

1. Delas Alas, J.G. and R.P. Encarnacion, 1984. A one-dimensional non-linear numerical model for storm surge prediction. *Nat. Appl. Sci. Bull.* 36, No. 34, 235–251.
2. Jelesnianski, C.P., 1965. A numerical calculation of storm tides induced by a tropical storm impinging on a continental shelf. *Mon. Wea. Rev.* 93, 343–358.
3. Martin, S.T., 1985. A storm surge model for Manila Bay. Unpublished Master's Thesis, University of the Philippines.
4. Murty, T.S., R.A. Flather and R.F. Henry, 1986. The storm surge problem in the Bay of Bengal. *Progress in Oceanography* 16, 195–233.
5. Roed, L.P. and C.K. Cooper, 1987. A study of various open bound ary conditions for wind-forced barotropic numerical ocean models. In: Three-dimensional models of marine and estuarine dynamics, 45. J.C.J. Nihoul and B.M. Jamart, editors. Elsevier, pp. 305–335.
6. Wu, J., 1982. Wind stress over sea surface from breeze to hurricane. *J. Geophys. Res.* 87, C12, 9704–9706.

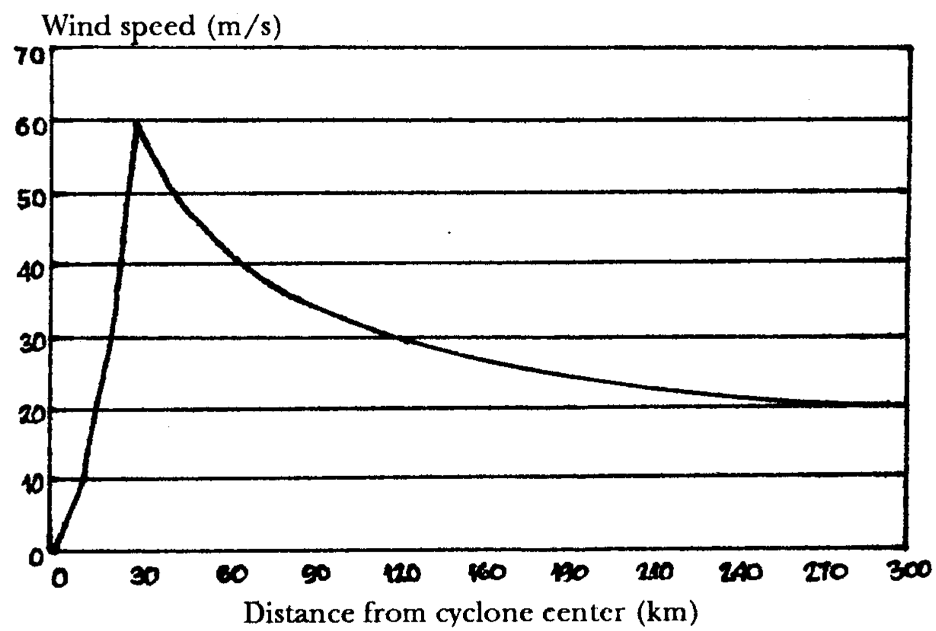
Wind speed (m/s)
70
60
50
40
30
20
10
0
0
30
60
90
120
160
190
210
240
270
300
Distance from cyclone center (km)

Figure 1

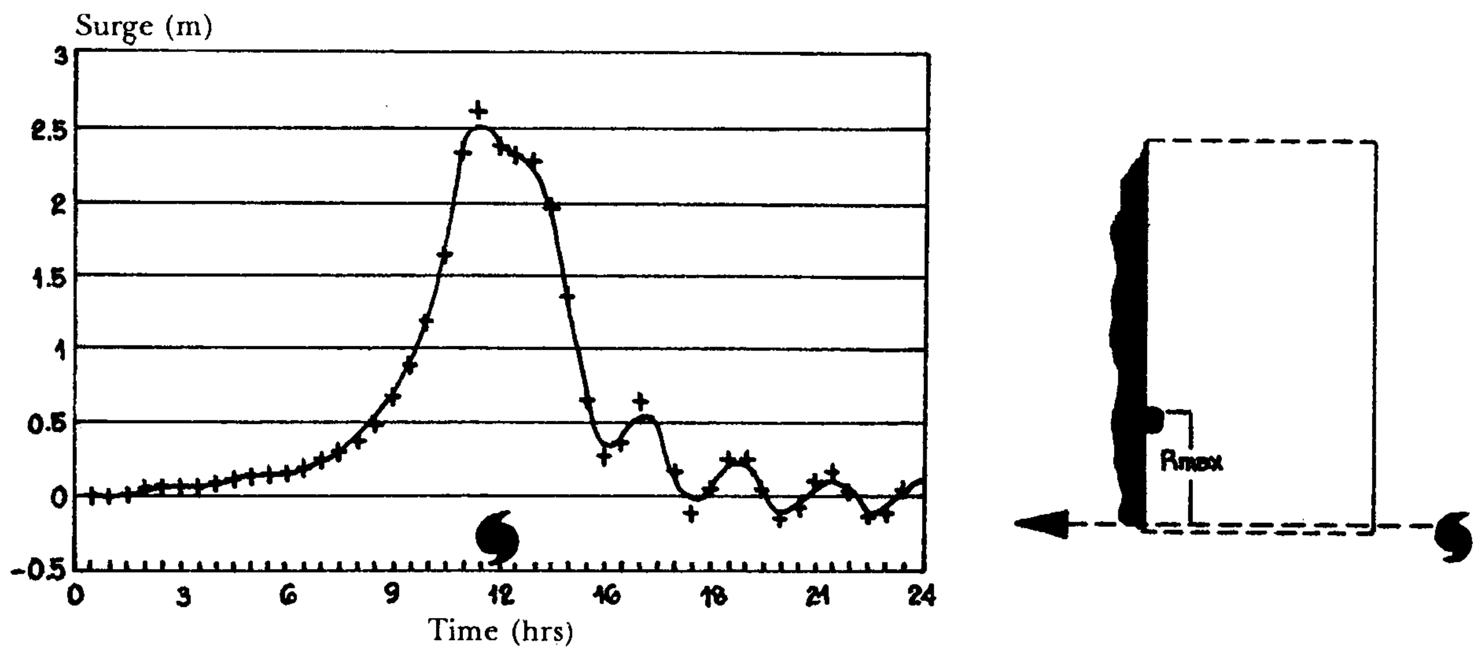

Figure 2a

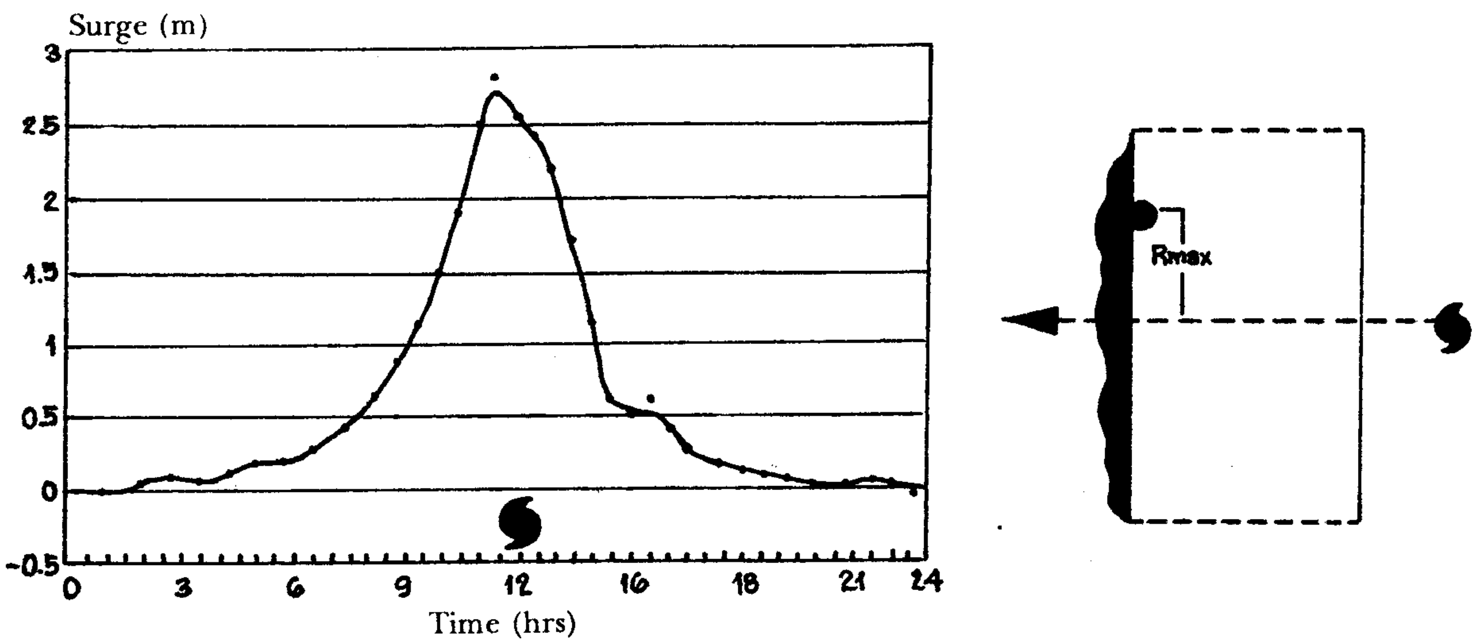

Figure 2b

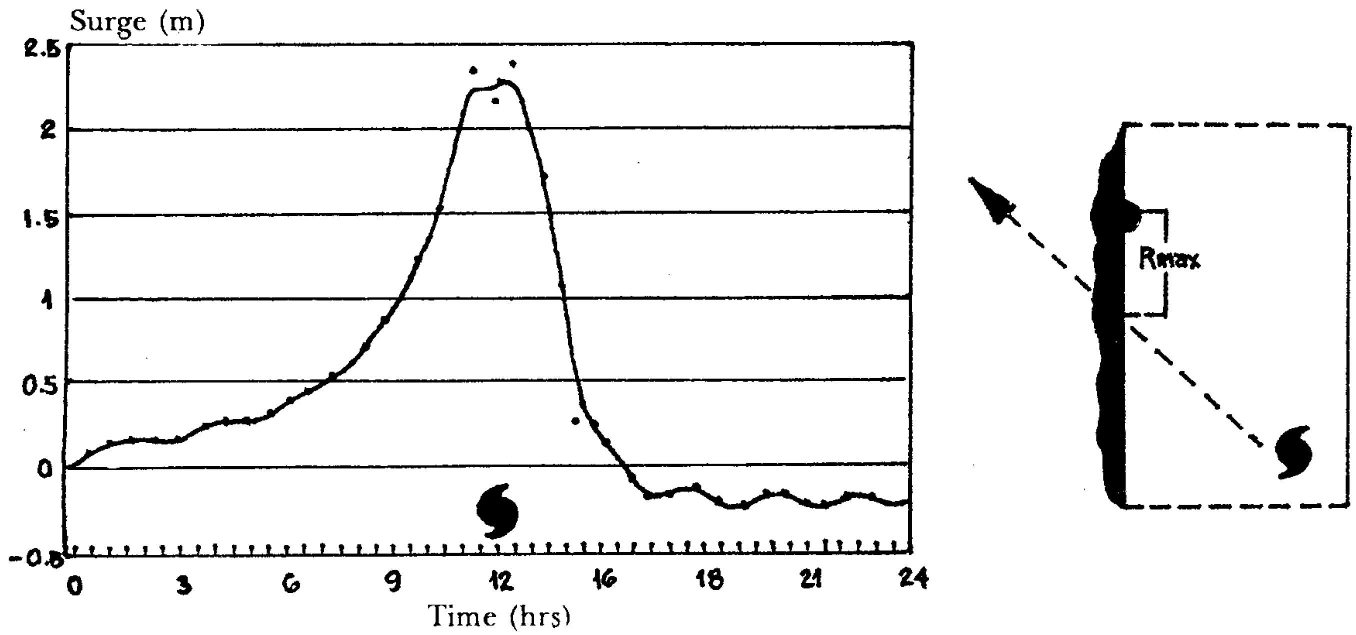

Figure 3a

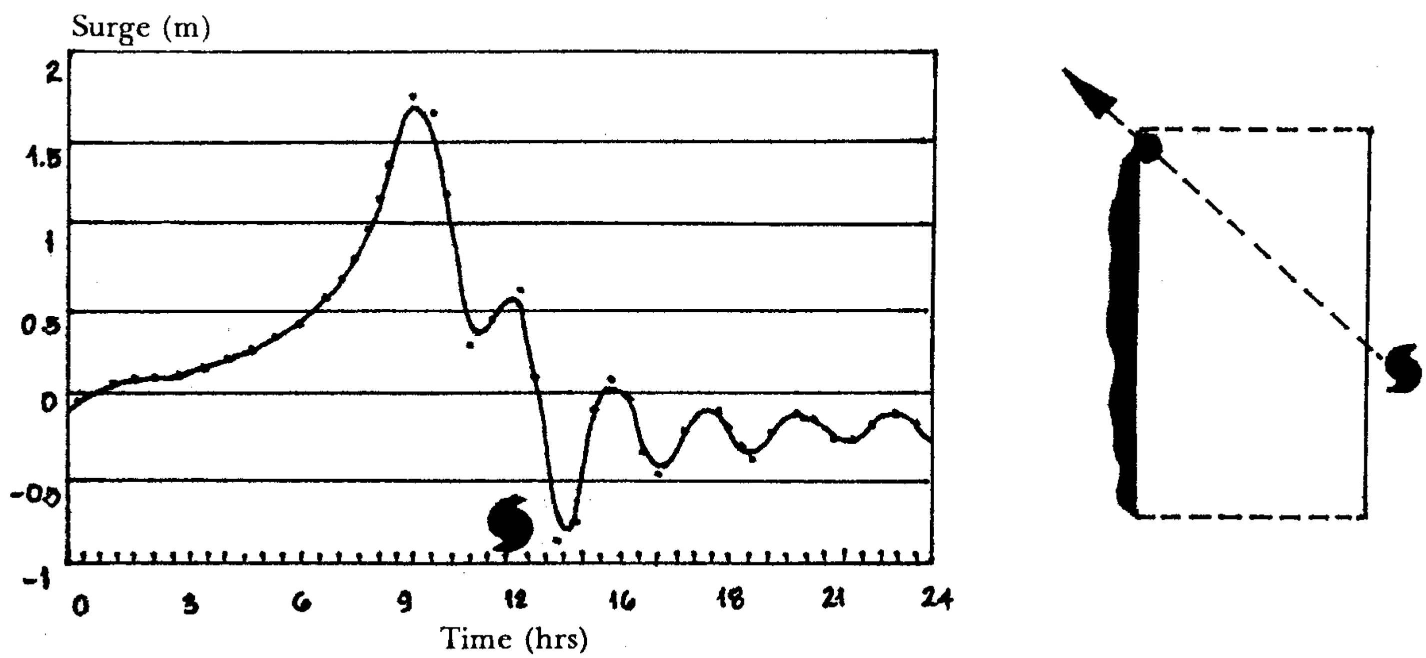

Figure 3b

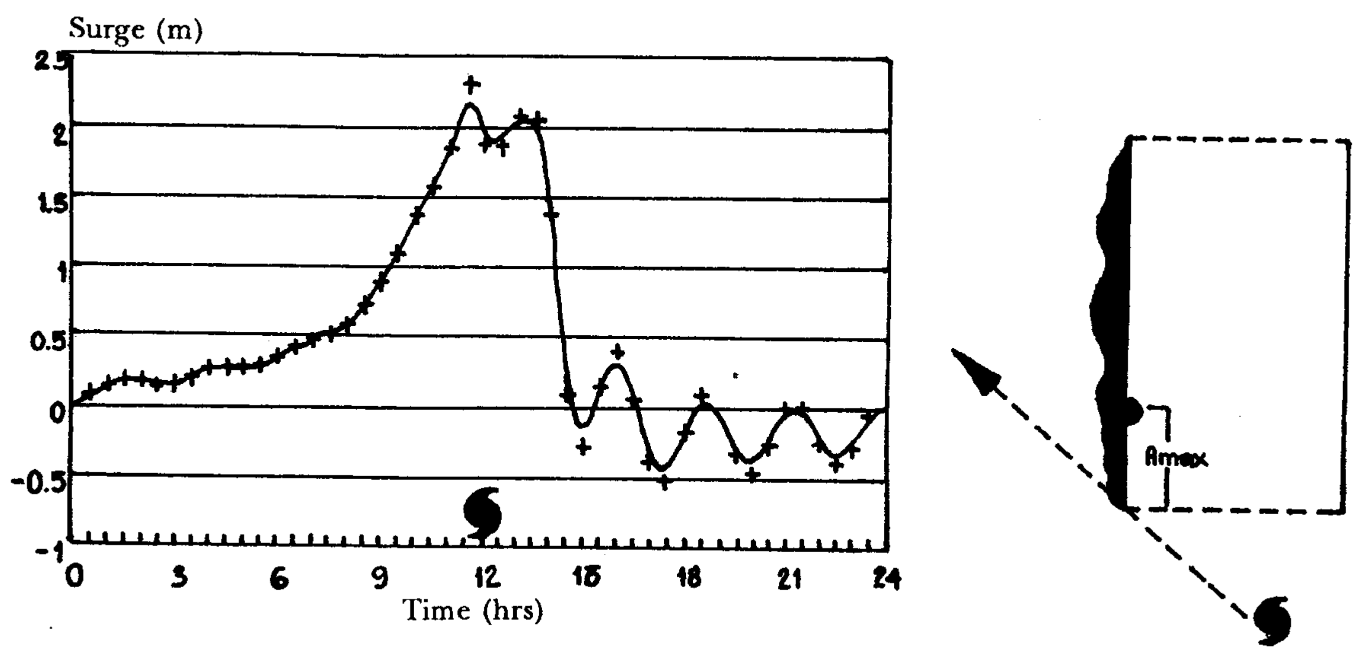

Figure 4a

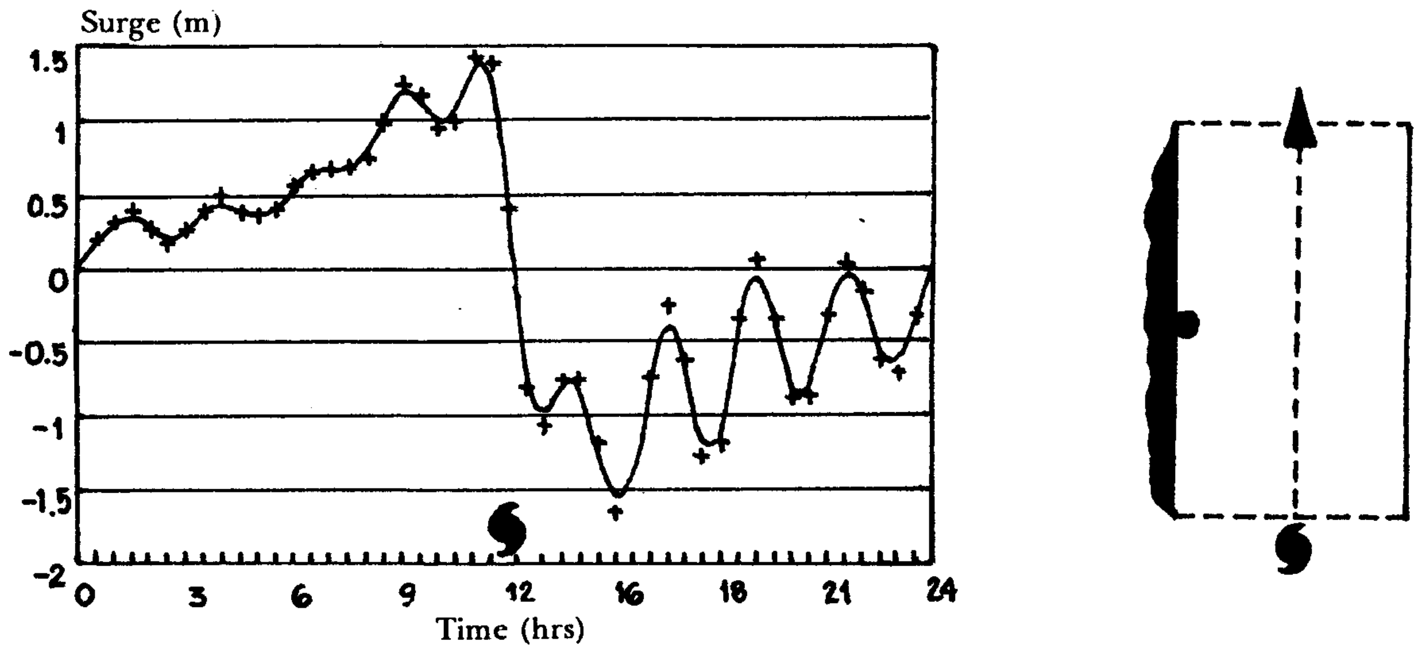

Figure 4b

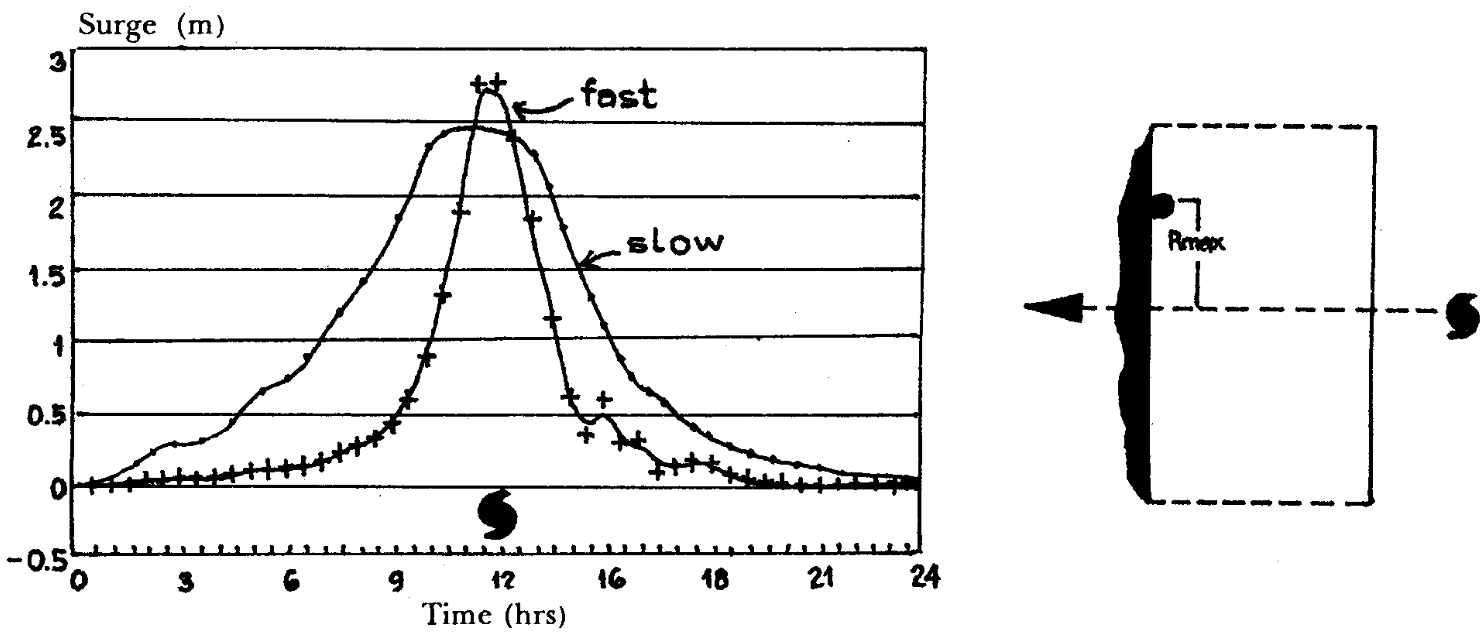
Surge (m)
3
2.5
2
1.5
1
0.5
0
-0.5
0
3
6
9
12
16
18
21
24
Time (hrs)
fast
slow
Rmax

Figure 5a

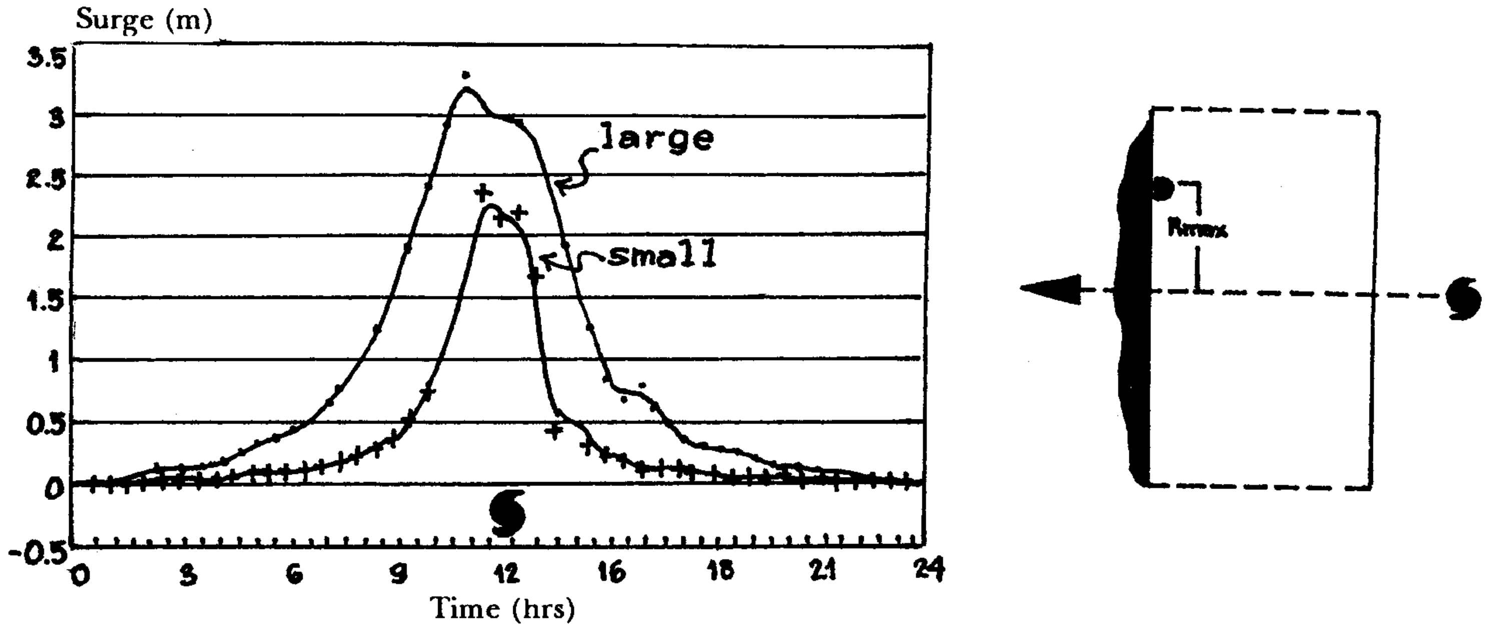
Surge (m)
3.5
3
2.5
2
1.5
1
0.5
0
-0.5
0
3
6
9
12
16
18
21
24
Time (hrs)
large
small
Rmax

Figure 5b

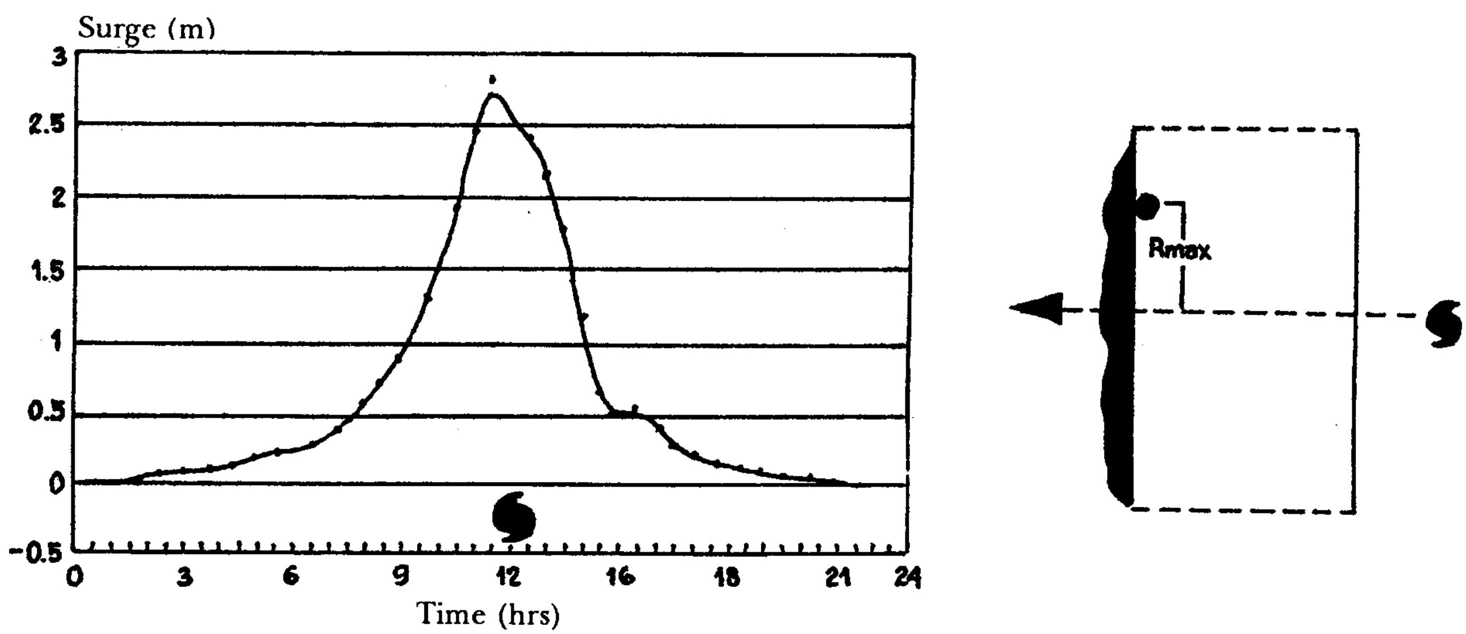

Figure 6a

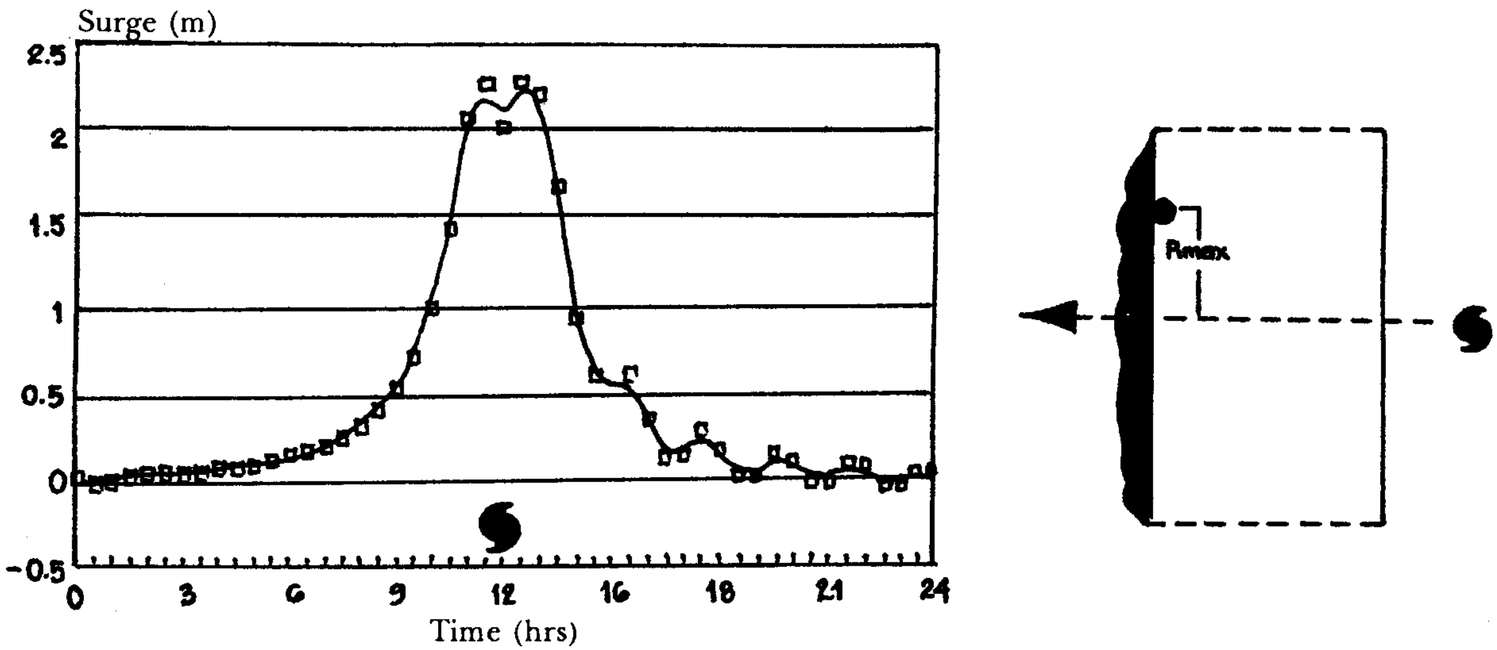

Figure 6b

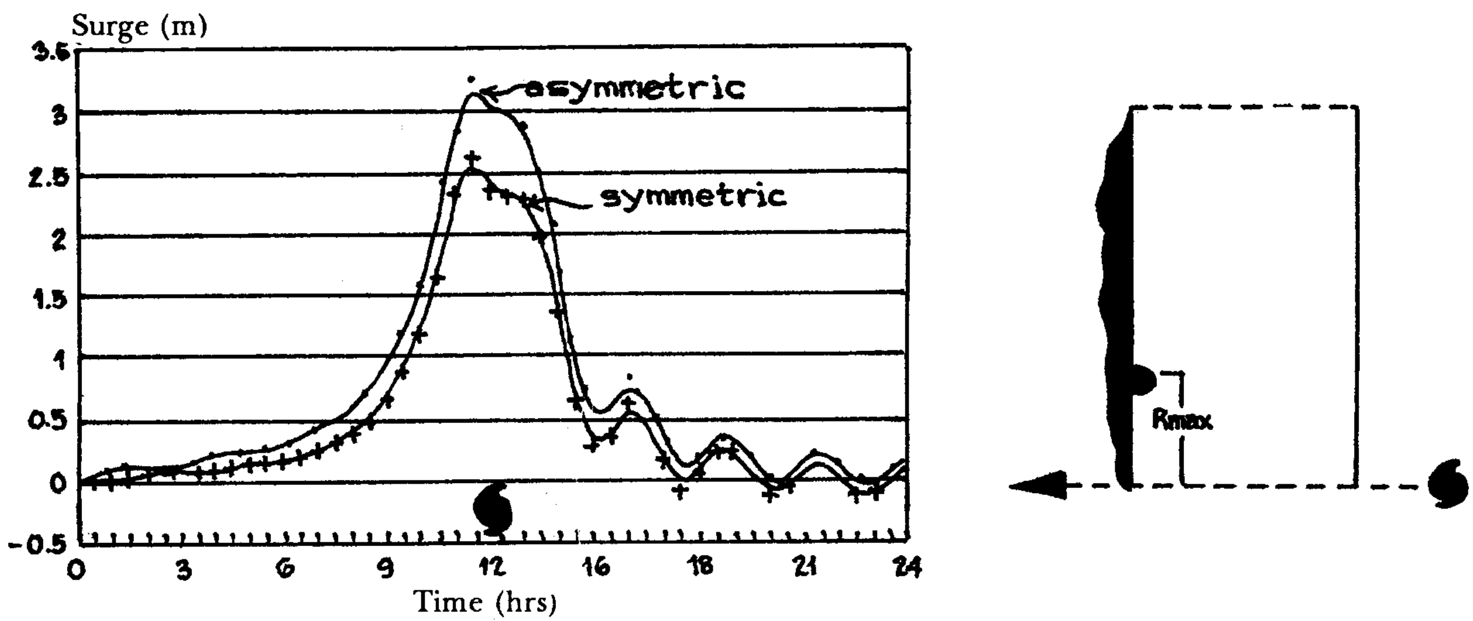
Surge (m)
3.5
3
2.5
2
1.5
1
0.5
0
-0.5
0
3
6
9
12
16
18
21
24
Time (hrs)
asymmetric
symmetric
Rmax

Figure 7a

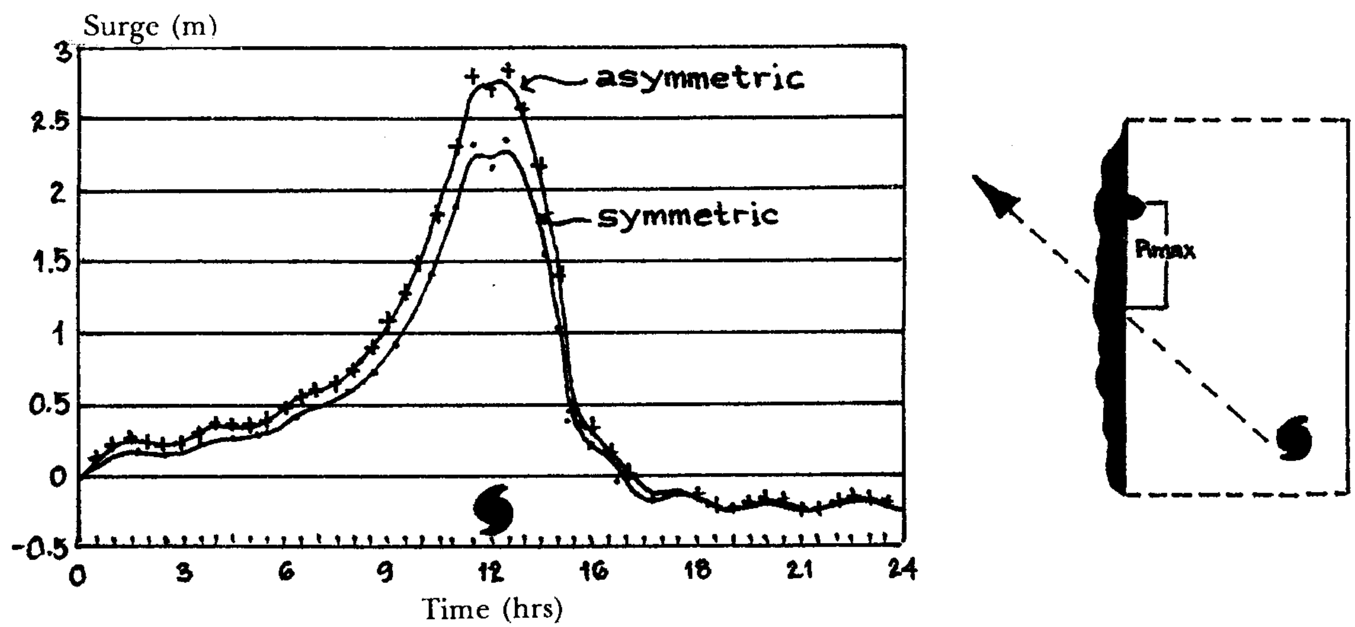
Surge (m)
3
2.5
2
1.5
1
0.5
0
-0.5
0
3
6
9
12
16
18
21
24
Time (hrs)
asymmetric
symmetric
Rmax

Figure 7b